Numerical Investigation of Dynamic Load Amplification in Buried Culverts

Mehdi Kadivar[1], Kalehiwot Nega Manahiloh[2], Victor N. Kaliakin[3], and Harry W. Shenton III[4]

ABSTRACT

Most traditional research on buried culverts has looked at live load distribution through soil onto buried culverts without due attention to the dynamic amplification of moving loads. Few studies that considered the dynamic amplification of buried culverts modeled the system assuming plane-strain conditions. Under such conditions, finite area loads such as the wheel loads of vehicles must instead be modeled as strip loads that act over the entire culvert width. In this study, the load-soil-culvert system is also treated as a three-dimensional problem. A dynamic amplification factor (*DAF*) is determined from two-dimensional (plane strain) and three-dimensional finite element analyses and is compared with *DAF*s calculated following the American Association of State Highway and Transportation Officials (AASHTO) procedures and field collected data. The two- and three-dimensional finite element analyses resulted in average *DAFs* of 1.10 and 1.03, respectively. Average *DAF*s from field and the AASHTO procedures were calculated to be 0.97 and 1.30, respectively. Overall, the AASHTO *DAF*s are the highest and the field *DAF*s are the lowest. The two-dimensional finite element results gave *DAF* values that are higher than the ones from three-dimensional analyses and field evaluated values. The *DAF* calculated from three-dimensional finite element analyses is the closest to the field measured *DAF*s.

KEY WORDS: buried culvert, dynamic amplification factor, load rating, finite element analysis, live load, load-soil-culvert interaction.

Citation Information: Please cite this work as follows

Kadivar, M., K.N. Manahiloh, V.N. Kaliakin, and H.W. Shenton, *Numerical Investigation of Dynamic Load Amplification in Buried Culverts.* Transportation Infrastructure Geotechnology, 2018. **5**(1): p. 24-41.

Link to the published work: https://link.springer.com/article/10.1007%2Fs40515-017-0045-7

---

[1] Graduate Student, Department of Civil and Environmental Engineering, University of Delaware, 301 DuPont Hall, Newark, DE 19716; email: mehdika@udel.edu.

[2] Corresponding Author, Assistant Professor, Department of Civil and Environmental Engineering, University of Delaware, 301 DuPont Hall, Newark, DE 19716; e-mail: knega@udel.edu, PH (302) 831-2485, FAX (302) 831-3640; ORCID: 0000-0003-3568-5110.

[3] Professor, Department of Civil & Environmental Engineering, University of Delaware, 301 DuPont Hall, Newark, DE 19716; email: kaliakin@udel.edu.

[4] Professor, Department of Civil & Environmental Engineering, University of Delaware, 301 DuPont Hall, Newark, DE 19716; email: shenton@udel.edu.

INTRODUCTORY REMARKS

Buried culverts are crucial components of the civil infrastructure in that they serve both structural and hydraulic purposes. Structurally they carry traffic loads. Hydraulically culverts help to safely channel water from the roadway.

The behavior of culverts is largely similar to that of bridges, except that they have shorter spans [1] and may have fill material placed on their top slab.

QUANTIFYING DYNAMIC RESPONSE OF CULVERTS

AASHTO considers the dynamic response of bridges and bridge-like structures such as culverts to be a function of the dynamic amplification factor (*DAF),* which is defined as follows:

$$DAF = \frac{R_{Dyn}}{R_{stat}} \quad (1)$$

where R_{Dyn} is some measure of the dynamic response of the structure, and R_{stat} is the same measure of the structure's static response.

For culverts with no fill material placed above the slab surface, AASHTO recommends a *DAF* value of 1.33 [2]. When fill is present, the *DAF* is decreased as a function of fill depth (D_E) according to

$$DAF = 1 + 0.33(1.0 - 0.125D_E) \geq 1 \quad (2)$$

where D_E is measured in feet. In AASHTO, the quantity [$0.33(1.0-0.125D_E)$] is referred to as the Impact Factor (*IM*).

The *DAF* is also used to calculate the rating factor (*RF*) from the following expression:

$$RF = \frac{C - \gamma_{DC}(DC) - \gamma_{DW}(DW) \pm \gamma_P(P)}{\gamma_{LL}(LL + DAF - 1)} \quad (3)$$

where C is the load carrying capacity of the culvert, and DC and DW are the dead loads due to component and to wearing surface and utilities, respectively. In Equation (3) LL is the live load and P is the permanent load. Finally, γ_{DC}, γ_{DW}, γ_{LL} and γ_{p} are the dead load components factor, the dead load wearing surface and utilities factor, the live load factor, and the permanent load factor, respectively.

The RF represents the current load carrying capacity of bridges and bridge-like structures such as culverts. RF value of less than one indicate that the structure does not meet the specified load carrying capacity.

BACKGROUND

The behavior of bridges and culverts subjected to dynamic loading has been rather widely investigated [e.g., 3,4-12]. Of particualr interest to the present discussion are findings related to the DAF.

Fleming and Romualdi [13] examined the effect of span length on the DAF and found that for bridges spanning less than 13 m, the AASHTO recommended DAF values were smaller than values measured in the field. For medium and large span bridges, Fleming and Romualdi [13] found the AASHTO recommended DAF values to be in accordance with field estimated values. Based on the findings of a more general study of the dynamic response of highway bridge structures, Smith [9] specified that DAF values were influenced by span length, vehicle speed, axle spacing, and the bridge's fundamental frequency.

Heins and Lee [14] performed in-situ load rating tests and two-dimensional finite element (FE) analyses of bridges. They reported a good agreement between FE simulated DAF values and those measured in-situ.

Coussy et al. [10] performed a theoretical study of the effects of random surface irregularities on the dynamic response of bridges subjected to moving loads. They concluded that *DAF* values decreased with span length.

Eymard et al. [3] modeled a bridge as an elastic beam and performed a dynamic analysis for a specified traffic load. Their results demonstrated that the behavior of bridges subjected to traffic loads can successfully be captured by the results of a single mode dynamic analysis.

Manko and Beben [15] investigated the effect that variations in vehicle speed, surface roughness, and vehicle braking have on the *DAF* of a 12.3 m span bridge. The *DAF* values obtained ranged from 1.15 to 1.20; these values are less than the aforementioned AASHTO recommended value of 1.33.

Wekezer et al. [6] also investigated the influence of different parameters on the dynamic reponse of bridges. They determined that this response is significantly dependent upon the span length, girder size, and natural frequency of the bridge. In addition, Wekezer et al. [6] investigated the effect that a bridge's road surface conditions have on its dynamic response. They concluded that a smooth approach surface can decrease the dynamic response by as much as 194%.

The dynamic response of culverts has not been studied nearly as extensively as that of bridges. The earliest work in this area appears to be that of Turneaure et al. [11], who reported a rather pronounced influence of a culvert's span length on the *DAF*. Spangler et al. [16] investigated the effect of vehicle loading, under both static and dynamic conditions, on the behavior of culverts. They attached strain gauges and measured not only strains but also displacements at different locations in the culvert. Spangler et al. [16] reported *DAF* values ranging between 1.11 and 1.29. More recently, Beben [17] observed that *DAF* values for culverts increased with span length and decreased with fill depth.

Beginning in the late 1960's, culverts were modeled mathematically as two-dimensional solution domains under the assumption of plane strain conditions and analyzed using the finite element method (FEM). Whereas early FE analyses focused primarily on circular [18-22] and elliptical [23] culverts, subsequent analyses have involved reinforced concrete box girders [24,25].

More recently, Chen and Harik [26] used a two-dimensional (plane strain) FE analysis to investigate the dynamic response of buried concrete culverts. The results of these analyses showed that increases in vehicle speed increased the *DAF* values, while increases in surface roughness decreased them. These results appear to contradict the aforementioned findings of [6].

Wells [27] also used two-dimensional FE analyses to examine the effect that variations in span length, slab thickness, soil fill depth, asphalt rigidity, and the soil's Young's modulus have on the *DAF* values for culverts. In addition to the aforementioned FE analyses, Wells [27] performed field load rating tests on five different culverts. Based on the FE results, as well as the field measurements, Wells [27] reported *DAF* values that were consistently less than the AASHTO recommended value of 1.33.

The two-dimensional (plane strain) modeling of culverts is relatively straightforward. In addition, the computational effort for two-dimensional FE analyses is appreciably less than for three-dimensional ones. There is, however, one potentially significant source of inaccuracy associated with plane strain idealizations of culverts. In such idealizations, the culvert is assumed to be loaded by applied surface forces that do not vary in the direction perpendicular to the plane containing the culvert cross-section. The actual forces are, however, typically applied to the culverts only over finite areas corresponding to the contact area associated with a vehicle's wheel. Since such loading violates the plane strain assumption, it follows that culverts should be modeled and analyzed as three-dimensional bodies.

Although the loading associated with a plane strain idealization is expected to give overly conservative *DAF* values, the ramifications of this assumption have not been investigated. This could partly be attributed to the preconceived notion that three-dimensional analyses are computationally intensive and impractical for routine load capacity assessments. This paper describes the results of two-dimensional (plane strain) and three-dimensional FE analyses of four culverts located in the state of Delaware. Calculated *DAF* values are compared with each other and with those estimated from field load rating tests and AASHTO procedures.

MATHEMATICAL MODELING AND NUMERICAL ANALYSIS OF CULVERTS

Description of Culverts

Four culverts, located in New Castle County of the state of Delaware, were mathematically modeled and analyzed using the FEM. In the subsequent discussion, these culverts are referred to as BR-1, BR-2, BR-3, and BR-4.

The dimensions of all four road-culvert-soil systems were measured in-situ. Cores were drilled at two opposite corners and at the center of each culvert. The average of all pertinent dimensions measured at these three locations was used in creating the associated mathematical models of the four road-culvert-soil systems.

Field explorations showed that culverts BR-1 and BR-2 have only a layer of asphalt on top of their top slab and no soil fill. In addition, these culverts do not have a bottom slab. Culverts BR-3 and BR-4, on the other hand, have bottom slabs, layers of soil, crushed stone and asphalt overlying their top slab. Culverts BR-1 and BR-2 had an inverted U-shaped cross-section, while the cross-section of culverts BR-3 and BR-4 was box-like. Figure 1 schematically shows one-half of the cross-section of culverts BR-1 and BR-2 in two- and three-dimensional views. Figure 2 shows the comparable information for culverts BR-3 and BR-4.

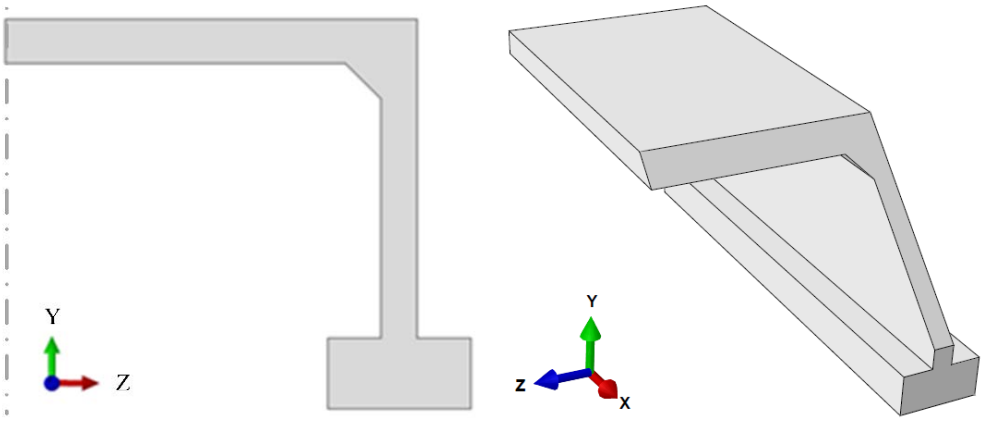

(a) (b)

Figure 1. Schematic illustration of one-half of the cross-section for culverts BR-1 and BR-2: (a) two-dimensional; (b) three-dimensional view.

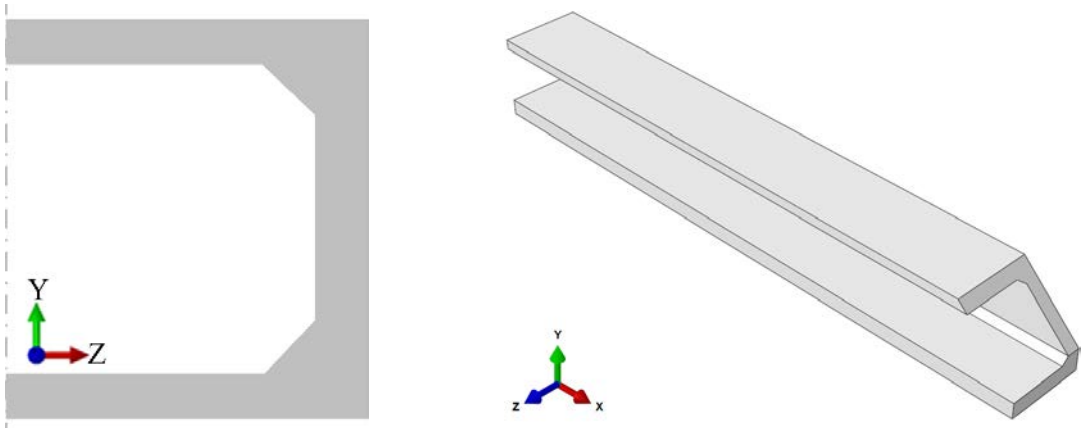

(a) (b)

Figure 2. Schematic illustration of one-half of the cross-section for culverts BR-3 and BR-4: (a) two-dimensional; (b) three-dimensional view.

Figure 3 schematically shows one-half of a typical road-culvert-soil system and its key dimensions. In Figure 3, the quantities $t_{(soil)}$, $t_{(stone)}$, and $t_{(asphalt)}$ represent the thickness of the soil fill, crushed stone, and asphalt, respectively. The quantities t_w, t_s, t_b, and t_t represent the thickness of the culvert wall, the culvert top slab thickness, the culvert bottom slab thicknesses, and the chamfer width, respectively. The quantity L_s is one-half of the culvert span length, H is the height

of the culvert, and *W* is the roadway width. Finally, *L* is the full longitudinal length of the modeled system, and *D* is the depth of the soil mass below the bottom of the culvert. Table 1 lists the dimensions measured in-situ for each of the four road-culvert-soil systems.

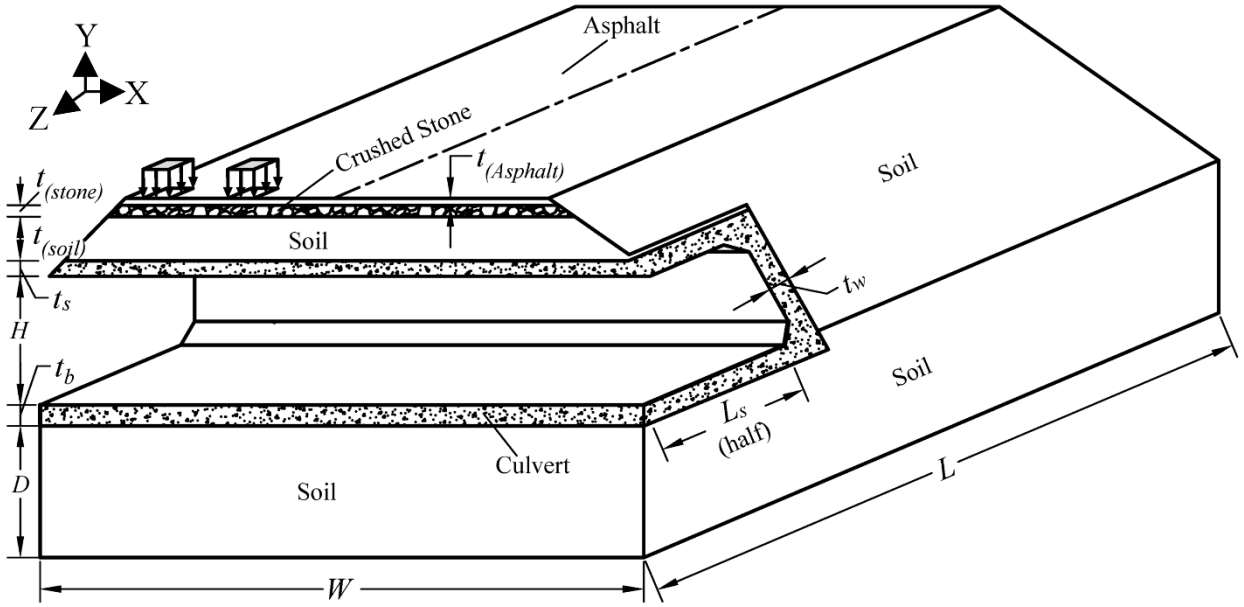

Figure 3. Schematic illustration of a typical road-culvert-soil system.

Table 1 Dimensions of the road-culvert-soil systems (all values are in meters).

Culvert	$t_{(soil)}$	$t_{(stone)}$	$t_{(asphalt)}$	t_w	t_s	t_b	t_t	L_s	H	W	L	D
BR-1	0	0	0.13	0.30	0.38	0	0.30	3.20	2.44	15.44	23.50	5.00
BR-2	0	0	0.13	0.30	0.38	0	0.30	3.86	4.04	21.24	24.16	5.00
BR-3	0.32	0.26	0.11	0.30	0.30	0.30	0.15	2.13	3.05	19.60	22.43	5.00
BR-4	0.25	0.20	0.13	0.30	0.30	0.36	0.15	1.52	1.88	28.50	21.82	5.00

Spatial Idealizations and Nodal Constraints

Using the aforementioned dimensions, all four road-culvert-soil systems were modeled both as two-dimensional (plane strain) and three-dimensional solution domains. Since all four road-culvert-soil systems were geometrically symmetrical with respect to the front plane, and because the applied loading was symmetrical with respect to the same plane, the solution domains consisted

of only one-half of the entire system. Figures 4 and 5 show typical two- and three-dimensional meshes, respectively.

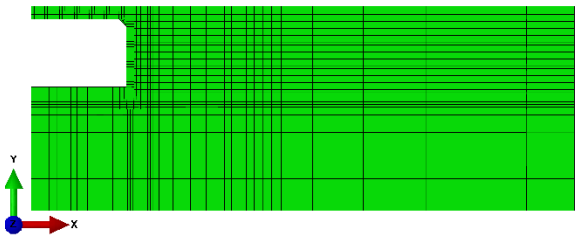

Figure 4. Typical mesh for two-dimensional finite element analyses.

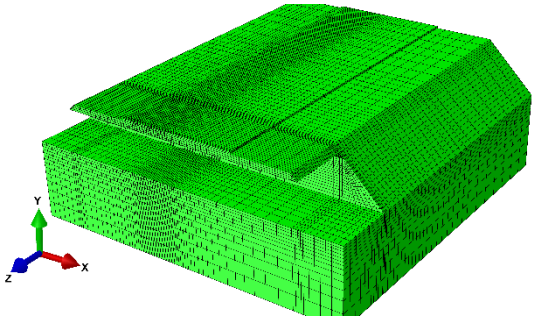

Figure 5. Typical mesh for three-dimensional finite element analyses.

In the two-dimensional solution domains, the left boundary is a plane of symmetry (Figure 4). Displacements normal to this plane (i.e., in the *x*-direction) were thus constrained through suitable nodal specifications. To ensure that the right boundary does not affect the static and dynamic response of the road-culvert-soil system, "infinite" elements [28] were placed along this boundary. These elements map to infinity in the *x*-direction and prevent rigid body displacements in this direction. For dynamic analyses "infinite" elements ensure that no artificial radiation will be simulated at this boundary. Similar elements were also placed along the bottom boundary of the two-dimensional solution domains. In this case the elements map to infinity and prevent rigid body displacements in the *y*-direction.

In the three-dimensional solution domains, the left boundary parallel to the *x*-*y* plane is a plane of symmetry (Figure 5). Displacements normal to this plane (i.e., in the *z*-direction) were thus

constrained. To ensure that the rear boundary parallel to the *x*-*y* plane does not affect the static and dynamic response of the road-culvert-soil system, “infinite” elements were placed along this boundary, thus preventing rigid body displacements in the *z*-direction. “Infinite” elements were also placed along the boundaries parallel to the *y*-*z* plane, thus preventing rigid body displacements in the *x*-direction. Finally, “infinite” elements were placed along the bottom *x*-*z* plane, thus preventing *y*-direction rigid body displacements were constrained along this boundary.

In summary, the use of “infinite” elements along all but the symmetry boundaries ensured that the road-culvert-soil systems analyzed were situated on a semi-infinite half-space. In this manner, the boundaries of the two- and three-dimensional solution domains will not affect the static and dynamic response of these systems.

The relative displacement between the materials on either side of their common interfaces requires the use of special interface elements. The importance of accounting for such relative displacements in the FE models of the road-culvert-soil systems was investigated in preliminary analyses. It was determined that the inclusion of interface elements had negligible effects on the results of the FE analyses. Consequently, no such elements were included in subsequent analyses of the road-culvert-soil systems. This significantly reduces the computational effort associated with such analyses.

Mesh Density and Extent

The asphalt, crushed stone, concrete and soil were discretized using quadrilateral and hexahedral continuum elements in the two- and three-dimensional models, respectively. In FE analyses, choosing the appropriate mesh size is requisite to obtaining accurate results. The proper extent of each mesh in the appropriate coordinate directions was determined through mesh sensitivity analyses. Based on the results of these analyses, the meshes extend approximately 20

m longitudinally and 5 m in depth. Any larger distances did not significantly affect the displacements and stresses in the vicinity of the applied load, especially in light of the fact that the aforementioned "infinite" elements were placed along the boundaries of the solution domain. The element size in this vicinity was on the order of 0.10 m. The size was then graded out to approximately 1.0 m at the furthest extent of the solution domain.

In two-dimensional analyses, the total number of nodes in a given mesh ranged between 2,000 and 4,000. In the three-dimensional analyses, the number of nodes ranged between 97,000 and 145,000. In two-dimensional analyses, the total number of elements in a given mesh ranged between 1,800 and 3,700. In the three-dimensional analyses, the number of elements ranged between 83,000 and 123,000.

Material Characterization and Parameter Values

The vehicle loads typically used in load rating tests produce very small displacements and deformations in the road base and in the culvert. Consequently, the asphalt, crushed stone, concrete, and soil were idealized as isotropic, linear elastic materials. Each of these materials is thus characterized by the values of the elastic modulus and Poisson's ratio. Table 2 lists the values of parameters used in all of the mathematical models analyzed; these values were taken from Wu et al. [29].

Table 2. Values of Material Parameters and Densities.

Material	Elastic Modulus (MPa)	Poisson's Ratio	Density (kg/m^3)	Damping constant α
Asphalt	1200	0.25	2400	0.40
Stone	250	0.35	2300	0.40
Concrete	31000	0.15	2400	0.05
Soil	50	0.40	1800	0.40

Applied Loading

Procedures stipulated by the AASHTO [2] standard specification were followed in applying all loads. As such, the loading was applied from the rear tire of a test truck [2,30]. The magnitude of the applied truck load on the pavement surface is 93 kN (21 kips). This load was divided between the two wheel sets of the rear tires that are 1.83 m (6') from each other (see Figure 6a). Each wheel touches the ground with a contact area of 0.25 m × 0.5 m (10" × 20"). The tire load was applied at the mid span of culverts, where the maximum deflection is expected. Figure 6b shows one of the test trucks employed in this work.

(a) (b)

Figure 6. Test truck: (a) cross-sectional dimensions; (b) picture taken during testing

In the field, static loads are applied by driving the test truck at crawling speeds (e.g., 5 mph). Dynamic loads are generated by driving the test truck at speeds of 20, 30, and 40 miles per hour. In the FE analyses, static and dynamic loads are differentiated by the duration of application of the maximum load. In static analyses, the load ramps to its maximum value and is maintained at this value for the entire duration of the analysis. By contrast, in dynamic analyses the load takes the form of the triangular pulse shown in Figure 7. The load thus quickly ramps up to its maximum value and then, just as quickly, decreases to zero. The total duration (i.e., t_d) of the dynamic load

(i.e., the time taken by the test truck to cross each culvert) is calculated by dividing the span length (i.e., $2L_s$) of each culvert by the appropriate speed used during field testing. Then, the dynamic load would take half of the total duration to attain its peak magnitude.

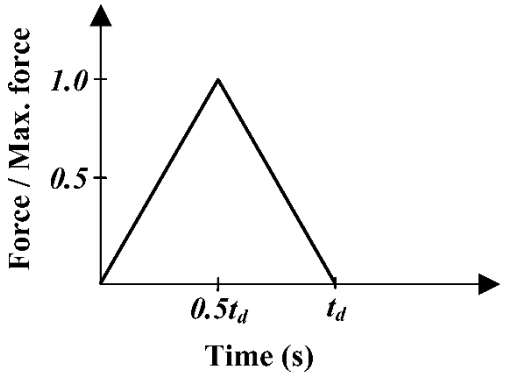

Figure 7. Typical dynamic load.

Algorithm for Dynamic Analysis

The dynamic FE analyses of the road-culvert-soil systems were performed using implicit direct integration in time. The specific solution scheme used was the so-called α-method proposed by Hilber et al. [31]. Three algorithmic parameters (α^*, β^*, and γ^*) are associated with this scheme. To introduce algorithmic damping and to retain unconditional stability while maintaining second-order accuracy, the range $-\frac{1}{3} \leq \alpha^* \leq 0$ is recommended [32], with

$$\gamma^* = \frac{1}{2}(1 - 2\alpha^*) \quad ; \quad \beta^* = \frac{1}{4}(1 - \alpha^*)^2 \tag{4}$$

A value of α^* equal to -0.05 was used in all of the dynamic analyses, thus ensuring some algorithmic damping. Using this value of α^* in Equations (4) gives γ^* = 0.55 and β^* = 0.2756.

The effects of possible physical damping were considered by introducing Rayleigh-type damping for each material. Values for the damping parameter (α) are listed in Table 2. For all the materials, the other damping parameter (β) were set to be zero [29].

Program and Computational Platform

All two- and three-dimensional FE analyses were performed using the ABAQUS® computer program [33], which was implemented on two computing platforms. The three-dimensional dynamic FE analyses were run on the University of Delaware parallel computing cluster system. This system consists of 200 computer nodes that total 5160 AMD "Interlagos" cores, 14.5TB of RAM, a 180TB Lustre filesystem, and a QDR InfiniBand network backplane. The three-dimensional static analyses, as well as all static and dynamic two-dimensional analyses were run on a personal computer with 3.6 GHz processor and 16 GB of random-access memory.

Average run time for a three-dimensional dynamic FE analysis on the cluster system was about two and half hours. By comparison, if these analyses were run on the aforementioned personal computer, the computational time would increase to an average of seven hours. On the personal computer, the three-dimensional static analyses took about 20 minutes to complete; all two-dimensional analyses were performed in under 1 minute.

RESULTS AND DISCUSSION

As previously noted, culverts BR-1 and BR-2 had similar (U-shaped) cross-sections and no fill soil. Culverts BR-3 and BR-4 also had similar (box-like) cross-sections and soil conditions. Due to their physical similarities, it is thus not surprising that culverts BR-1 and BR-2 behaved in a similar fashion, and that culverts BR-3 and BR-4 likewise behaved similarly. The simulated static and dynamic response of each of these two culvert pairs is now discussed.

Results from Two-dimensional FE analyses

Figures 8a and 8b show the displacement time histories computed at a critical node[5] in the two-dimensional (plane strain) dynamic FE analysis of culverts BR-1 and BR-2, respectively. For these culverts, the maximum displacements occurred 0.25 and 0.30 seconds after load application, respectively. Figures 9a and 9b show similar displacement time histories for culverts BR-3 and BR-4. For both culverts, the maximum displacements occurred 0.17 and 0.12 seconds after initiation of loading, respectively.

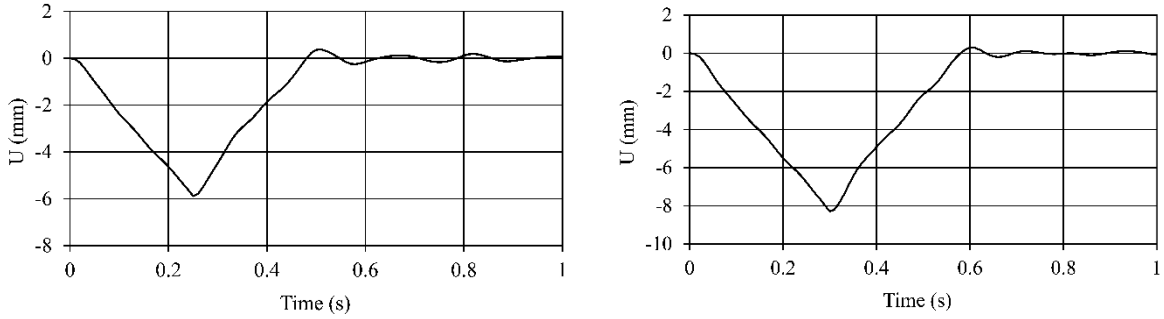

(a) (b)

Figure 8 Displacement time history for a critical node in a two-dimensional FE analysis: a) Culvert BR-1; b) Culvert BR-2

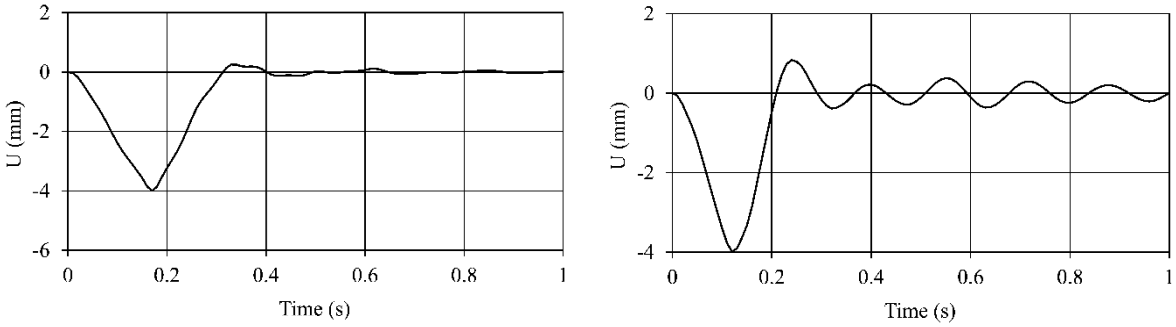

(a) (b)

[5] A "critical node" is the node, in the FE model, where the maximum deflection was recorded.

Figure 9 Displacement time history for a critical node in a two-dimensional FE analysis: (a) Culvert BR-3; (b) Culvert BR-4

Figures 10 and 11 show stress and displacement contours for culverts BR-1 and BR-2, respectively, at peak response during dynamic and static loading. Figures 11 and 12 show similar contours for culverts BR-3 and BR-4. To facilitate visualization, the response is magnified by a factor of 100. In these figures, the maximum compressive stresses are found at the top surface of the top slab, just under the loading surface, and at the inner top corner of the culvert. The maximum tensile stress is found at the inner surface of the top slab. This location also corresponds to the location at which the maximum displacement is recorded. From the contour plots it can also be observed that no change in stress distribution occurs beyond the 20 m length and 5 m depth model boundaries that were set following a mesh sensitivity analysis.

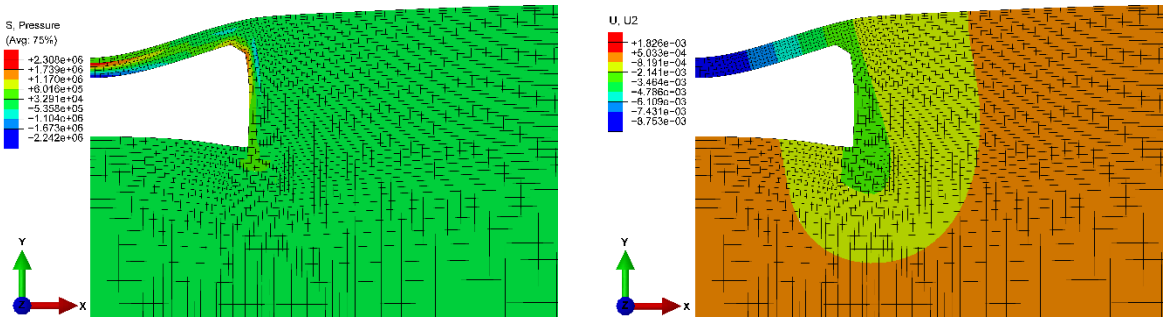

(a) (b)

Figure 10 Typical peak dynamic response in two-dimensional FE analysis of culverts BR-1 and BR-2 (magnified 100 times): (a) Stress contour (N/m^2); (b) Displacement contour (m).

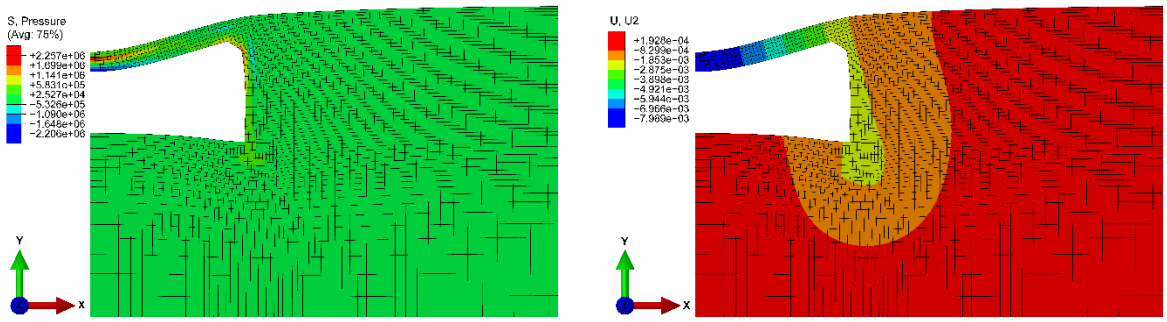

(a) (b)

Figure 11 Typical peak static responses in two-dimensional FE analysis of culverts BR-1 and BR-2 (magnified 100 times): (a) Stress contour (N/m^2); (b) Displacement contour (m).

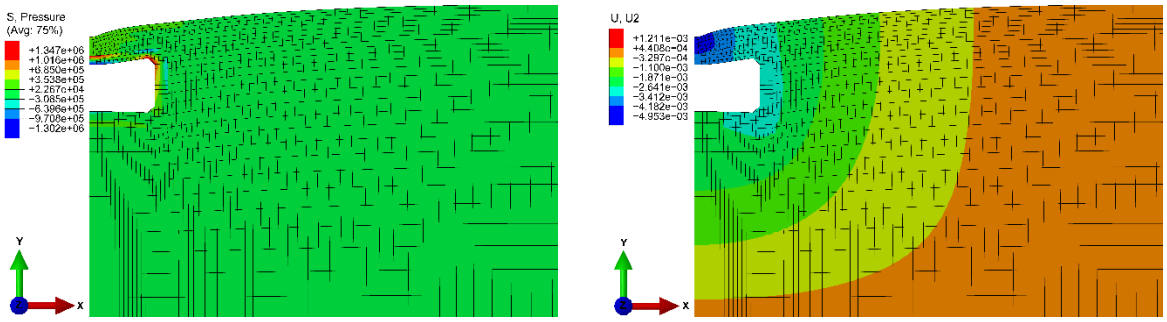

(a) (b)

Figure 12 Typical peak dynamic responses in two-dimensional FE analysis of culverts BR-3 and BR-4 (magnified 100 times): (a) Stress contour (N/m^2); (b) Displacement contour (m).

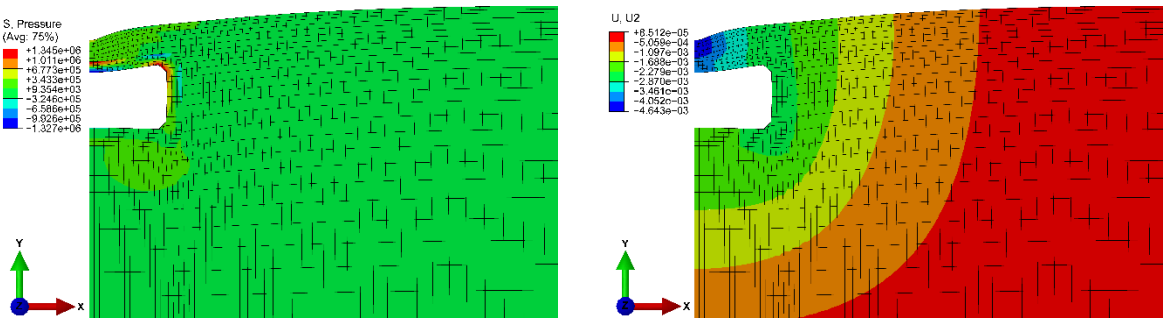

(a) (b)

Figure 13 Typical peak static response in two-dimensional FE analysis of culverts BR-3 and BR-4 (magnified 100 times): (a) Stress contour (N/m^2); (b) Displacement contour (m).

Comparing the static and dynamic response for each of the two culvert pairs, it is evident that the stress and displacement contours have similar shapes. The magnitude of stresses and displacements generated under dynamic conditions are slightly larger than those associated with static loading.

Results from Three-Dimensional FE Analyses

As noted in the Background discussion, two-dimensional (plane strain) FE modeling of road-soil-culvert systems is relatively straightforward and computationally less intensive than three-dimensional analyses. The loading associated with a plane strain idealization does not, however, represent the actual truck wheel loads that are applied over their contact areas. In addition, two-dimensional FE models cannot account for all aspects of the of road-soil-culvert geometry. For example, the shoulder slope and the inclined culvert boundaries cannot be accounted for in a plane strain idealization. Three-dimensional FE analyses thus minimize the number of assumptions made in modeling of road-soil-culvert systems.

Figures 14a and 14b show the displacement time histories computed at a critical node in the three-dimensional dynamic FE analysis of culverts BR-1 and BR-2, respectively. For these culverts, the maximum displacements occurred 0.25 and 0.30 seconds after load application, respectively. These values are identical to those obtained in the plane strain FE analysis of culverts BR-1 and BR-2 (recall Figures 8a and 8b).

Figures 15a and 15b show similar displacement time histories for culverts BR-3 and BR-4. For both of these culverts, the maximum displacements occurred 0.17 and 0.12 seconds after initiation of loading, respectively. These values are once again identical to those obtained in the plane strain FE analysis of culverts BR-3 and BR-4 (recall Figures 9a and 9b).

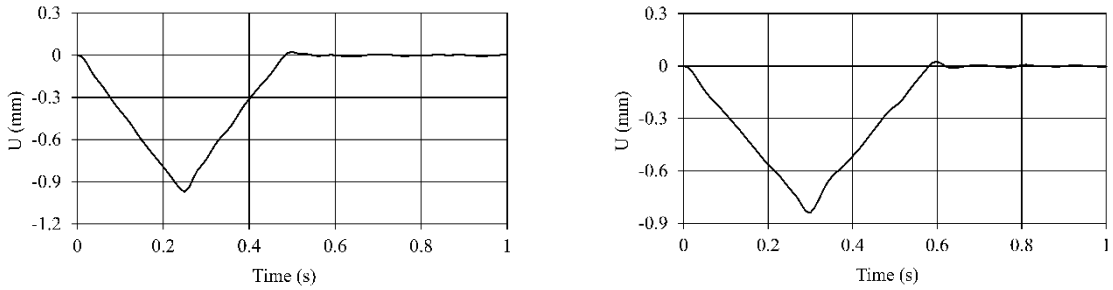

(a) (b)

Figure 14 Displacement time history for a critical node in a three-dimensional FE analysis: a) Culvert BR-1; b) Culvert BR-2.

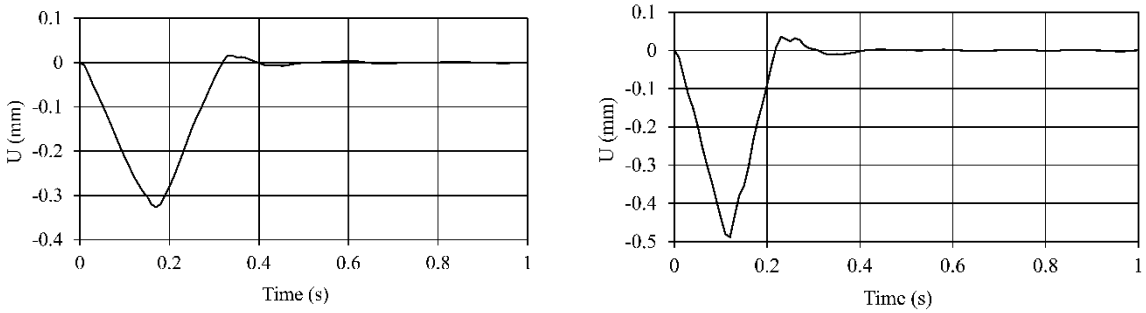

(a) (b)

Figure 15 Displacement time history for a critical node in a three-dimensional FE analysis: a) Culvert BR-3; b) Culvert BR-4.

Figures 16 and 17 show stress and displacement contours for culverts BR-1 and BR-2, respectively, at peak response during dynamic and static loading. Figures 18 and 19 show similar contours for culverts BR-3 and BR-4. To facilitate visualization, the response is magnified by a factor of 400. Similar to the two-dimensional FE analyses, the maximum compressive stresses are found at the top surface of the top slab, just under the loading surface, and at the inner top corner of the culvert.

The maximum tensile stress is found at the inner surface of the top slab. This location also corresponds to the location at which the maximum displacement is recorded.

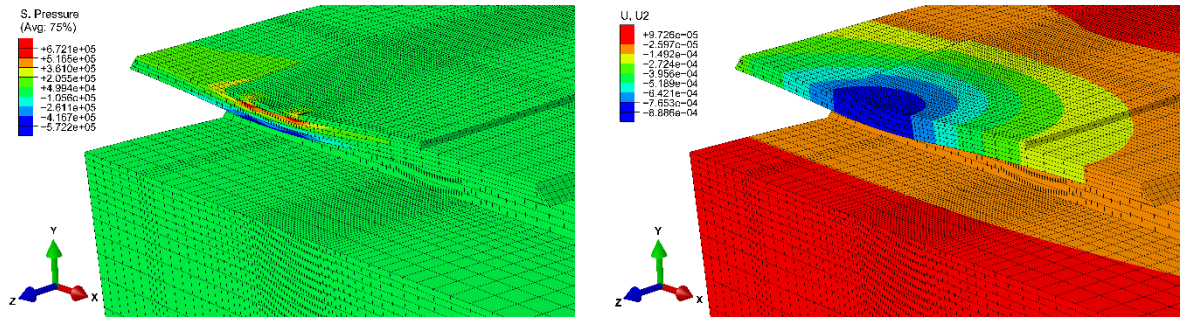

(a) (b)

Figure 16 Typical peak dynamic response in three-dimensional FE analysis of culverts BR-1 and BR-2 (magnified 400 times): (a) Stress contour (N/m^2); (b) Displacement contour (m).

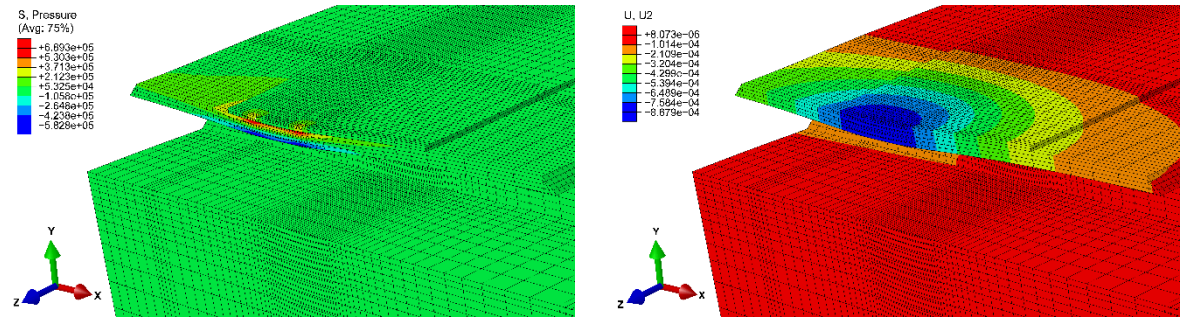

(a) (b)

Figure 17 Typical peak static response of three-dimensional FE analysis of culverts BR-1 and BR-2 (magnified 400 times): (a) Stress contour (N/m^2); (b) Displacement contour (m).

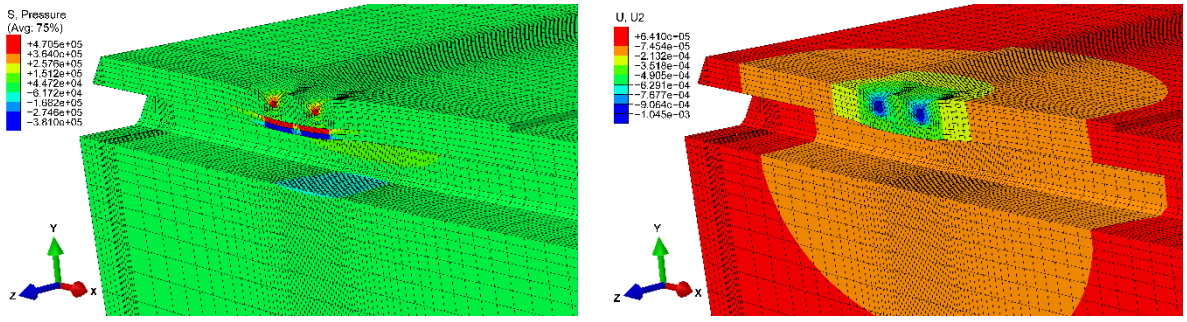

(a) (b)

Figure 18 Typical peak dynamic response of three-dimensional FE analysis of culverts BR-3 and BR-4 (magnified 400 times): (a) Stress contour (N/m^2); (b) Displacement contour (m).

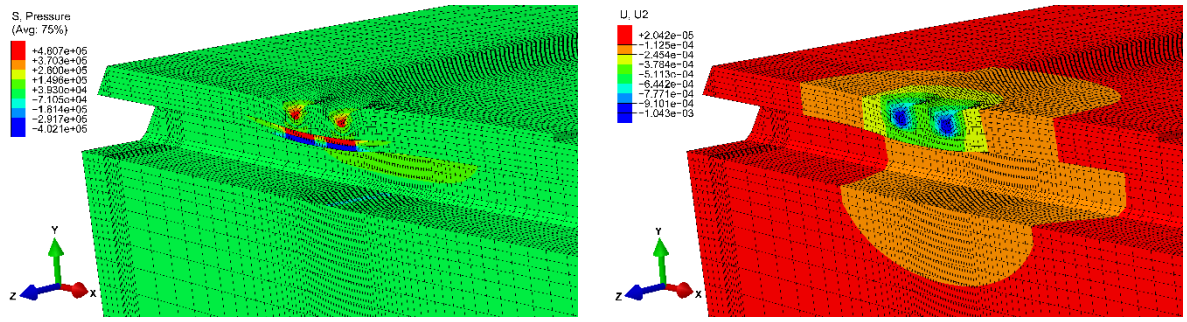

(a) (b)

Figure 19 Typical peak static response of three-dimensional FE analysis of culverts BR-3 and BR-4 (magnified 400 times): (a) Stress contour (N/m^2); (b) Displacement contour (m).

As noted in discussing the results of the two-dimensional FE analyses, the stress and displacement contours have similar shapes. The magnitude of stresses and displacements generated under dynamic conditions are slightly larger than those associated with static loading. Both of these conclusions likewise hold for the results of the three-dimensional FE analyses.

Summary of the FE analyses

Table 3 summarizes the maximum displacements computed in the two- and three-dimensional static and dynamic FE analyses. Also listed in this table are *DAF* values computed for each of the four culverts in two- and three-dimensional analyses. On average, the maximum displacements from the two-dimensional FE analyses are more than eight times greater than comparable values computed in three-dimensional analyses. This large difference is explained by the fact that in plane strain analyses, the loading is assumed to be continuous (into the plane), as opposed to the actual wheel loads that are applied (over finite areas) in three-dimensional analyses. Finally, the *DAF* values associated with the two-dimensional FE analyses are all larger than comparable values computed in three-dimensional analyses.

Table 3 Summary of maximum displacements and related DAF values.

Culvert	Two-Dimensional FE Analysis			Three-Dimensional FE Analysis		
	Static (mm)	Dynamic (mm)	*DAF*	Static (mm)	Dynamic (mm)	*DAF*
BR-1	5.661	5.883	1.04	0.961	0.972	1.01
BR-2	7.966	8.300	1.04	0.840	0.840	1.00
BR-3	3.710	3.998	1.08	0.315	0.327	1.04
BR-4	3.608	3.989	1.11	0.479	0.488	1.02
Average	5.236	5.542	1.07	0.649	0.657	1.02

DAF values from field measurements and AASHTO procedures

For culverts BR-3 and BR-4, where a layer of backfill is present, AASHTO recommended *DAF* values are computed using Equation (2). For culverts BR-1 and BR-2, where no backfill is present, AASHTO recommends a *DAF* value of 1.33.

Field computed *DAF* values for culverts BR-1 to BR-4 are taken from [27]. In these field studies, the dynamic displacement was measured when the rear axle of the standard truck crossed the mid-span of the culvert, at speeds exceeding 25 mph. The actual speed of the truck was decided based on roadway conditions. For static displacement measurements, the truck was driven at a "crawling" speed of 5 mph. Figure 20 shows typical sensors used to measure field displacements.

Figure 20 Typical displacement sensor layout.

Table 4 summarizes *DAF* values calculated from field measurements and AASHTO procedures. On average, the AASHTO recommended *DAF* values were 33.85% larger than the field calculated values.

The *DAF* values obtained from two-dimensional FE analyses ranged from 1.06 to 1.11. All two-dimensional *DAF*s were larger than field *DAF*s, with minimum and maximum deviations of 4.95% and 20.65%, respectively. The *DAF* values from the two-dimensional FE analyses were, however, smaller than the AASHTO *DAF*s.

Among all *DAF* values, those obtained from three-dimensional FE analyses were the closest to the field measured values. The three-dimensional *DAF*s ranged from 1.02 to 1.07, with minimum and maximum deviations of 1.98% and 16.30%, respectively, from the corresponding field values.

In light of the *DAF* values presented in Table 3 and 4, the AASHTO procedure for computing such values was found to be overly conservative. Two-dimensional FE models, even though not as accurate as those of the three-dimensional ones, gave *DAF*s that were in better agreement with values measured in the field, when compared to those of AASHTO *DAF*s.

Table 4 Field measurements and AASHTO recommended *DAF* values.

Culvert	AASHTO	Field
BR-1	1.33	1.01
BR-2	1.33	0.96
BR-3	1.25	0.92
BR-4	1.27	0.98
Average	1.30	0.97

CONCLUSIONS AND RECOMMENDATIONS

Load rating tests are expensive to run on a regular basis. They usually require traffic diversion and road blockage to avoid test disturbances. In light of these inconveniences, *DAF*s are commonly calculated analytically using the AASHTO provisions. Following the results observed in this study, it is recommended to use three-dimensional FE modeling to determine *DAF*s numerically. The modeling aspects and the computational time involved in running three-dimensional FE analyses are not as intensive as one might think. Once a working model is developed, the analysis takes a matter of a few hours to complete.

In cases where three-dimensional FE analysis could not be justified, the two-dimensional FE analysis should be used. Even though two-dimensional FE models did not capture the real culvert behavior, their *DAF* results have been found more accurate than those obtained from AASHTO procedures. The displacements obtained in the two-dimensional FE analyses were conservative, relative to the three-dimensional analysis results. Lastly, it is concluded that the

asphalt-culvert-soil interaction can more accurately be captured using three-dimensional FE analyses, where the least amount of simplification is required.

ACKNOWLEDGEMENTS

The authors are grateful for the financial support provided by the Delaware Department of Transportation. Any opinions, findings, and conclusions expressed herein are those of the authors and do not necessarily reflect the views of the Delaware Department of Transportation.

REFERENCES

1. FHWA: Recording and coding guide for the structure inventory and appraisal of the nation's bridges. In. United States Department of Transportation, Washington, DC., (1995)
2. AASHTO: LRFD Bridge Design Specifications, 6th Edition, with 2012 and 2013 Interim Revisions. In. American Association of State Highway and Transportation Officials, Washington, D.C., (2012)
3. Eymard, R., Guerrier, F., Jacob, B.: Dynamic behaviour of bridges under full traffic. Paper presented at the Eighth ASCE Structures Congress, Baltimore, MD, April 30-May 3
4. McLean, D.L., Marsh, M.L.: Dynamic Amplification Factors for Bridges. In: Board, T.R. (ed.) Synthesis of Highway Practice 266. Washington, D.C., (1998)
5. Deng, L., Yu, Y., Zou, Q., Cai, C.S.: State-of-the-Art Review of Dynamic Impact Factors of Highway Bridges. Journal of Bridge Engineering **20**(5) (2015). doi:doi:10.1061/(ASCE)BE.1943-5592.0000672
6. Wekezer, J., Taft, E., Kwasniewski, L., Earle, S.: Investigation of impact factors for FDOT bridges. (2010)
7. Tilly, G.P.: Dynamic Behaviour of Concrete Structures. In: Report of the RILEM 65 MDB Committee. Amsterdam; New York, (1986)

8. Bakht, B., Pinjarkar, S.G.: Review of dynamic testing of highway bridges. In., vol. SRR-89-01. (1989)

9. Smith, K.N.: Dynamic behaviour of highway bridge structures. In: Interim Report, Ontario Joint Highway Research Programme. vol. Project C-1. (1969)

10. Coussy, O., Said, M., Van Hoore, J.P.: The influence of random surface irregularities on the dynamic response of bridges under suspended moving loads. Journal of Sound and Vibration **130**(2), 313-320 (1989).

11. Turneaure, F.E., Crandall, C.L., Cartlidge, C.H., Schneider, C.C.: Report of Sub-committee on Impact. In: Twelfth Annual Convention, American Railway Engineering and Maintenance o Way Association 1911

12. Dhar, C.L., Chu, K.H., Garg, V.K.: DYNAMIC RESPONSE OF A SINGLE TRACK RAILWAY TRUSS BRIDGE. Paper presented at the Bridge Engineering Conference, 1st, St Louis, Missouri, USA,

13. Fleming, F.J., Romualdi, J.P.: Dynamic response of highway bridges. ASCE Journal of the Structural Division **87**(7), 31-60 (1961).

14. Heins, C.P., Lee, W.H.: Curved box-girder bridge: field test. ASCE Journal of the Structural Division **107**(2), 317-327 (1981).

15. Manko, Z., Beben, D.: Dynamic testing of a corrugated steel arch bridge. Canadian Journal of Civil Engineering **35**(3), 246-257 (2008). doi:10.1139/L07-098

16. Spangler, M.G., Mason, C., Winfrey, R.E.: Experimental determinations of static and impact loads transmitted to culverts. In: Mason, C.W., Winfrey, R.E. (eds.). Iowa State College, Ames, Ia., (1926)

17. Beben, D.: Dynamic amplification factors of corrugated steel plate culverts. Engineering Structures **46**, 193-204 (2013). doi:http://dx.doi.org/10.1016/j.engstruct.2012.07.034

18. Brown, C.B., Green, D.R., Pawsey, S.: Flexible culverts under high fills. Journal of the structural devision **94**(4), 905-918 (1968).

19. Duncan, J.M.: Behavior and design of long-span metal culvert structures. Journal of Geotechnical Engineering **105**(3), 399-418 (1979).

20. Katona, M.G.: CANDE: a versatile soil-structure design and analysis computer program. Journal of Advances in Engineering Software **1**, 3-9 (1978).

21. Roschke, M., Davis, R.E.: Rigid Culvert Finite Element Analysis. Journal of Geotechnical Engineering(ASCE) **112**(8), 749-767 (1986).

22. Wenzel, T., Parmelee, R.: Computer-Aided Structural Analysis and Design of Concrete Pipe. In: Bealey, M., Lemons, J. (eds.) Concrete Pipe and The Soil-Structure System. ASTM International, West Conshohocken, PA, (1977)

23. Abel, J.F., Mark, R., Richards, R.: Stresses Around Flexible Elliptic Pipes. Journal of the Soil Mechanics and Foundations Division **99**(7), 509-526 (1973).

24. Garg, A.K., Abolmaali, A.: Finite-Element Modeling and Analysis of Reinforced Concrete Box Culverts. Journal of Transportation Engineering **135**(3) (2007). doi:10.1061/(ASCE)0733-947X(2009)135:3(121)

25. Pimentel, M., Costa, P., Felix, C., Figueiras, J.: Behavior of Reinforced Concrete Box Culverts under High Embankments. Journal of Structural Engineering (ASCE) **135**(4) (2009). doi:10.1061/(ASCE)0733-9445(2009)135:4(366)

26. Chen, S.S., Harik, I.E.: Dynamic Effect of a Moving Truck on a Culvert. Journal of Bridge Engineering **17**(2) (2012).

27. Wells, A.: Analytical and Experimental Investigation of Dynamic Amplification Factor for the Load Rating of Reinforced Concrete Box Culverts. University of Delaware (2016)

28. Bettess, P.: Infinite Elements. International Journal for Numerical Methods in Engineering **11**(1), 53-64 (1977).

29. Wu, J., Liang, J., Adhikari, S.: Dynamic response of concrete pavement structure with asphalt isolating layer under moving loads. Journal of Traffic and Transportation Engineering (English Edition) **1**(6), 439-447 (2014). doi:http://dx.doi.org/10.1016/S2095-7564(15)30294-4

30. AASHO: The AASHO Road Test. In: Report 4, Highway Research Board, Special Report 61D. Washington, D.C., (1962)

31. Hilber, H.M., Hughes, T.J.R., Taylor, R.L.: Improved Numerical Dissipation for Time Integration Algorithms in Structural Dynamics. Earthquake Engineering and Structural Dynamics **5**(3), 283-292 (1977).

32. Hughes, T.J.R.: The Finite Element Method, Linear Static and Dynamic Finite Element Analysis. Prentice-Hall, New Jersey (1987)

33. ABAQUS: ABAQUS 6.14 Complete Abaqus Environment (CAE) online documentation. In, vol. https://www.3ds.com/products-services/simulia/products/abaqus/abaquscae/. Dassault Systems, Waltham, MA., (2014)